Charge Delocalization and Enhanced Acidity in Tricationic Superelectrophiles

Rajasekhar Reddy Naredla,[†] Chong Zheng,[†] Sten O. Nilsson Lill,[‡] and Douglas A. Klumpp*,[†]

[†]Department of Chemistry and Biochemistry, Northern Illinois University, DeKalb, Illinois 60115, United States
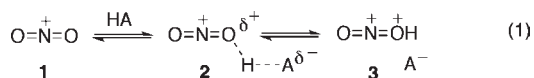[‡]Department of Chemistry, University of Gothenburg, SE-412 96 Gothenburg, Sweden

S *Supporting Information*

ABSTRACT: This Article presents the results from studies related to the chemistry of tricationic superelectrophiles. A series of triaryl methanols were ionized in Brønsted superacids, and the corresponding tricationic intermediates were formed. The trications are found to participate in two types of reactions; both are characteristic of highly charged organic cations. One set of reactions occurs through charge migration. A second set of reactions occurs through deprotonation of an unusually acidic site on the tricationic species. One of the tricationic intermediates has been directly observed by low temperature NMR spectroscopy. These highly charged ions and their reactions have also been studied using density functional theory calculations. As a result of charge migration, electron density at a carbocation site is found to increase with progression from monocationic to pentacationic structures.
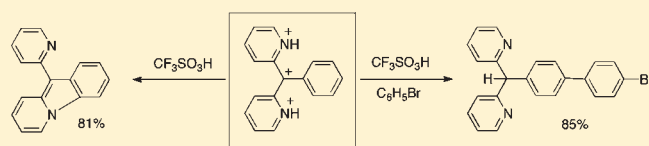
INTRODUCTION

During the mid-1970s, Olah proposed the concept of super-electrophilic activation.[1] Several published studies had previously described the high reactivities of monocationic electrophiles in superacidic media. This suggested that the monocationic electrophiles were interacting with the acidic media to enhance their reactivities. Thus, protonation of a monocationic species such as the nitronium ion (**1**) could produce an ion with an increasing positive charge (**2**, eq 1). In the limiting cases, even dicationic species (**3**) are considered to be involved in the chemistry. While many examples of dicationic superelectrophiles have been described,[2] few examples of tricationic species have been studied. Most tricationic and tetracation species are formed as resonance stabilized ions.[3] Little is known about the reactivities of small organic ions bearing such a large amount of positive charge.[4] In this Article, we describe studies in which a reactive carbocation site interacts with two adjacent cationic charges. Reactions of the tricationic species with arenes lead to products consistent with charge migration. Under some conditions, these reactive intermediates undergo cyclizations to produce novel heterocyclic ring systems. The tricationic intermediates are further studied by spectroscopic and theoretical methods.

$$O=\overset{+}{N}=O \underset{}{\overset{HA}{\rightleftharpoons}} O=\overset{+}{N}=O^{\delta+} \underset{H\cdots A^{\delta-}}{\rightleftharpoons} O=\overset{+}{N}=\overset{+}{O}H \quad A^- \qquad (1)$$

$$\mathbf{1} \qquad\qquad \mathbf{2} \qquad\qquad\qquad \mathbf{3}$$

RESULTS AND DISCUSSION

Our studies began with an examination of the chemistry of triarylmethanols (**4**−**8**, **14**, **15**) by reaction in superacidic CF$_3$SO$_3$H (Table 1). The triarylmethanol substrates were prepared readily from reactions of the appropriate ketones or esters with organolithium reagents. Two types of conversions were observed, depending on whether benzene was present in the mixture. In the presence of C$_6$H$_6$, alcohol **4** gives product **9** in 89% yield at 60 °C (entry 1). If the reaction was done at lower temperatures, then the starting material was recovered. Similar results were obtained with imidazole and benzimidazole-based substrates (**5**, **7**, **8**; entries 2, 4, 5). When the reaction was done with a substrate (**6**) bearing the 2-naphthyl substituent, nucleophilic attack occurred at the C-1 position of the naphthyl ring to give product **11** in good yield. The structure of compound **11** was established by ^{1}H and ^{13}C NMR spectra, mass spectrum analysis, and X-ray crystallography.[5]

In the absence of benzene, reactions of the triarylmethanols lead to cyclization products (entries 6−10). For example, compound **4** reacts in CF$_3$SO$_3$H at 60 °C to provide the pyrido[1,2-a]indole derivative (**16**) in 81% yield. Benzimidazole derivatives **5**, **6** also react to give cyclization products (**17** and **18**). In the reaction of **6**, cyclization occurs regioselectively at the 1-position of the naphthyl ring to give product **18** (confirmed by X-ray crystal structure).[5] The pyrido[1,2-a]indole derivatives **19** and **20** were formed by reactions of compounds **14** and **15**, respectively. Product **20** is the only major product from **15**, indicating a preference for cyclization at the pyridine ring. The vinyl-substituted derivative (**21**) does not undergo cyclization in CF$_3$SO$_3$H; however, a low yield of cyclization product (**22**) may be obtained from reaction in the stronger acid system CF$_3$SO$_3$H−SbF$_5$ (ca. 10:1; eq 2). These types of cyclizations involving *N*-heterocycles are not well-known, as the only other example was described by

Table 1. Reactions of Heterocyclic Alcohols in CF_3SO_3H at 60 °C (with and without C_6H_6)

| Entry	Starting material	Product with C_6H_6	Yield	Entry	Starting material	Product without C_6H_6	Yield
(1)	4	9	89%	(6)	4	16	81%
(2)	5	10	90%	(7)	5	17	91%
(3)	6	11	91%	(8)	6	18	92%
(4)	7	12	95%	(9)	14	19	88%
(5)	8	13	96%	(10)	15	20	82%

Posselt (involving cyclization between a 4-methoxyphenyl group and a pyridine or pyridinium ring).[6] Nevertheless, our results indicate that novel heterocyclic ring systems are prepared by the superacid promoted cyclizations of the triarylmethanols.

(2)
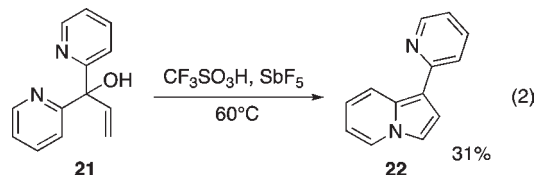
When triarylmethanols **23** or **24** are reacted under similar conditions, the carbocations **25** and **26** are produced (Figure 1). However, with benzene, no Friedel−Crafts products are formed from the monocation **25** or dication **26**. With simple heating to 60 °C (no benzene), cyclization products are also not obtained.[7] Compound **4** generates the tricationic intermediate **27** in heated superacid. Thus, trication **27** exhibits enhanced reactivity as compared to **25** and **26**. When substrate **4** is reacted with sub-stituted arenes, product formation (**28**−**30**) occurs with good regioselectivity. Reaction of compound **4** with toluene in CF_3-SO_3H gives **28** as the major product, isolated in 72% yield. Gas chromatography analysis of the crude product mixture indicated a para,ortho/meta ratio of about 10:1. A competition experiment was also done with substrate **4** in a CF_3SO_3H-promoted reaction with toluene/benzene (1/1 ratio). Analysis of the product mixture

showed high selectivity for the toluene with k_t/k_b of about 30:1. Similar results are obtained from reactions of **4** with bromo-benzene and 4-(3-phenylpropyl)pyridine. Products **29** and **30** are formed in good yields with high regioselectivities.

In addition to arene nucleophiles, we also attempted to capture the electrophilic intermediate(s) with n-type nucleophiles, in-cluding carbon monoxide, fluoride, and water. Although carbon monoxide often reacts efficiently with carbocationic intermediates,[8] no adducts of this nucleophile could be isolated in reactions with **4** in superacid. When compound **4** is reacted in CF_3SO_3H and KHF_2 is added, then fluoride adduct **31** may be isolated in 51% yield (eq 3; compound **4** is also recovered). Interestingly, nucleophilic attack occurs at the methine carbon rather than at the ring carbon. A similar reaction of **4** with CF_3SO_3H, followed by water, leads to formation of the starting material **4**, rather than functionalization at the remote position.

(3)
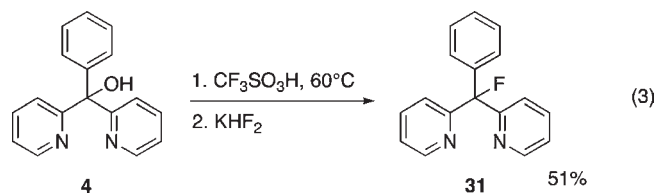
In our mechanistic studies, the intermediates and transition states were studied using density functional theory (DFT).

Geometries for these structures were initially optimized in the gas phase at the M06/6-31G(d) level of theory[9] using Jaguar.[10] Gibbs' free energy corrections (ΔG) were calculated, and structures were verified to be minima or transition states by inspection of the number of imaginary frequencies. In a second step, single-point energies of the optimized structures were calculated using M06/cc-pVTZ(-f),[11,12] giving a basis set correction term (ΔBS). In a final step, solvent phase geometry optimizations were done. Using a Poisson–Boltzmann solver as implemented in Jaguar,[13] electrostatic solvation effects from the surroundings were calculated using the SCRF method with CF_3SO_3H as a solvent (dielectric constant = 77.4, probe radius = 2.5985274).[14] The free energy (ΔG) and basis set correction terms (ΔBS) were added to the solution phase energy. NMR chemical shifts were calculated using B3LYP/IGLO-II as implemented in Gaussian 03,[15–17] on M06/6-31G(d) gas-phase optimized structures with benzene set to the experimental value of 127.7 ppm as the NMR reference. NBO charges were calculated using NBO 5.0 as implemented in Jaguar.[18] To verify that the M06/6-31G(d) compounds were able to properly describe the σ- and π-complexes, tests were also performed using B3LYP-DCP/6-31+G(d,p),[19,20] a dispersion-corrected DFT method, resulting in optimized structures similar to those with M06/6-31G(d).
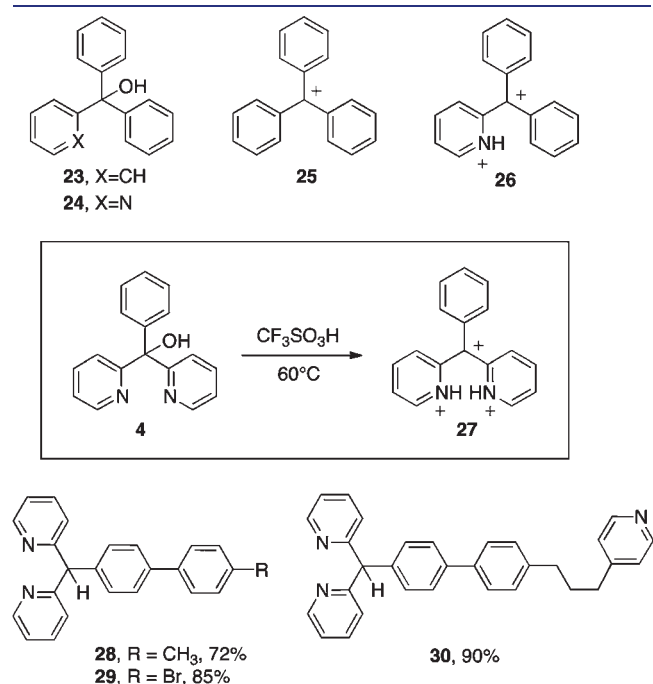

Figure 1. Ionization products (**25**–**27**) and Friedel–Craft reaction products **28**–**30**.

In considering the mechanisms of the reactions, we propose a mechanism involving formation of tricationic intermediates with highly delocalized carbocation centers and equilibria with a dicationic species from deprotonation. The alcohol substrates (**4**–**8**) react with benzene in the superacid, and nucleophilic attack occurs at the remote position on the aryl substituent group (Figure 2). Thus, compound **4** ionizes in superacid, and loss of water produces the tricationic superelectrophile **27**. With formation of the carbocation **27**, positive charge is highly delocalized into the adjacent phenyl ring. Nucleophilic attack occurs at the remote position on the phenyl group to give intermediate **32**, when benzene is present in the reaction mixture. Several examples of charge migration and remote functionalization have previously been reported involving dicationic superelectrophiles.[21]

Product **31** is formed by fluoride attack at the methine carbon, suggesting that some positive charge remains at the methine center. This raises an obvious question: why would the n-type nucleophiles (fluoride and water) react at the methine carbon while π-type nucleophiles (benzene and substituted arenes) react at the remote para-position of the phenyl group? First, there is likely some degree of steric effects influencing the regiochemistry of nucleophilic attack. Nucleophilic attack at the methine carbon (by benzene) would form the highly congested tetraarylmethane. Second, formation of the π-complex may enhance charge separation (Figure 3). Formation of the toluene π-complex (**33a**), and subsequent Wheland intermediate or σ-complex (**34a**), effectively moves the positive charge away from the pyridinium rings. Density functional theory (DFT) calculations were done (vide infra) and showed the toluene ring bears +0.62 charge in the π-complex (**33a**) and +0.97 charge in the σ-complex (**34a**). In the case of toluene, steric effects in the π-complex may also be important in the high para selectivity.[22]

Although high positional selectivity is often due to a large energy barrier between the π-complex and σ-complex,[23] this does not appear to be the case with **33a** and **34a**. DFT calculations have indicated that the π-complex resides in a very shallow potential energy well, as small perturbations in structure **33a** easily lead to formation of the σ-complex **34a** as found by DFT geometry optimizations. In the competition experiment, high substrate selectivity was observed ($k_t/k_b \approx 30:1$). This value likely reflects the relative stabilities of the σ-complexes with benzene and toluene.[23] When the π- and σ-complexes are examined, the σ-complex from toluene (**34a**) is 7.9 kcal mol^{-1} more stable than the π-complex from toluene (**33a**), while the σ-complex from benzene (**34b**) is only 4.6 kcal mol^{-1} more stable than its π-complex with benzene (**34a**).

In reactions of compound **6**, products **11** and **18** were formed. While charge migration occurred into the napthyl ring system, it did not delocalize to the most remote position (across both rings). Ionization of the benzimidazole rings and the hydroxy group leads to trication **35a** (eq 4). Formation of product **11**
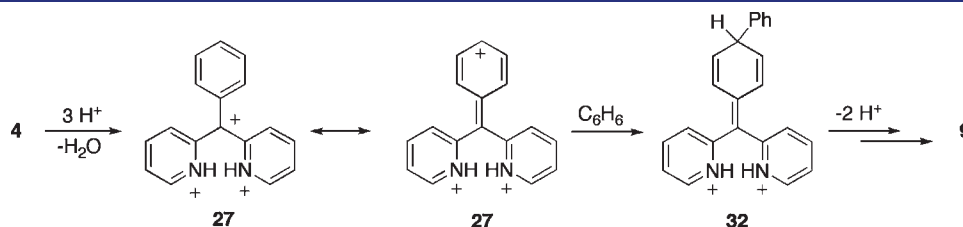
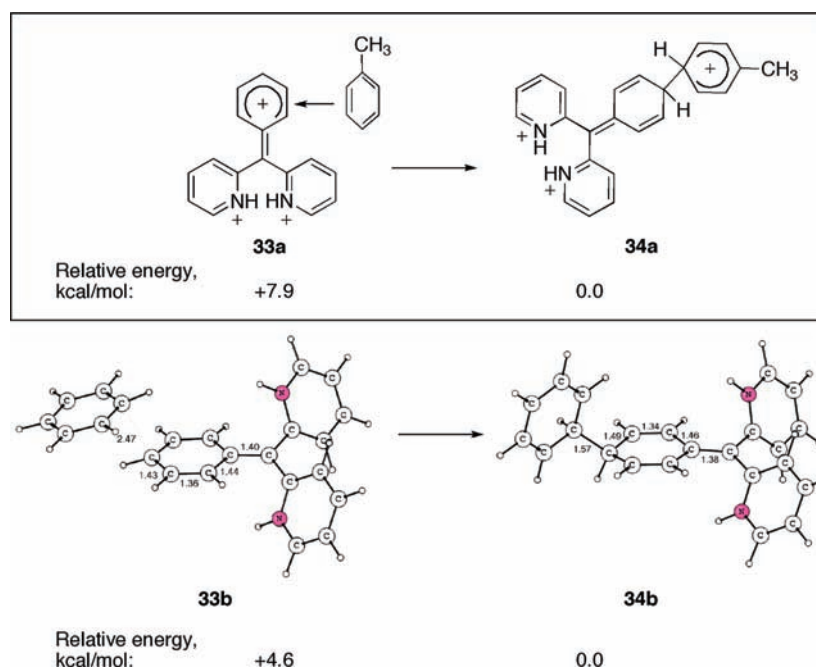**Figure 2.** Proposed mechanism for the reactions of trication **27**, leading to product **9**.

Figure 3. Relative energies of Wheland- and π-complexes with toluene (**33a**, **34a**) and benzene (M06/6-31G*-optimized structures, **33b**, **34b**).

Table 2. Observed ^{13}C NMR Data from Isoelectronic Carbocations 25−27 and Calculated ^{13}C NMR Data for 25−27 and 36,37[a]

A, B, C, D	Structure	Charge	^{13}C NMR data from FSO₃H-SbF₅-SO₂ClF	Calculated ^{13}C NMR data: C-methine, C-ipso, C-ortho, C-meta, C-para
CH, CH, CH, CH	25[a]	1+	211.6 (C+), 144.1,143.3,140.6, 131.1	205.1, 138.3, 142.2, 129.5, 144.4
NH+, CH, CH, CH	26[b]	2+	192.7 (C+), 149.9, 148.4, 145.2, 144.1, 137.9, 137.8, 133.0, 132.1, 132.1	184.3, 136.5, 144.3, 134.7, 157.0
NH+, NH+, CH, CH	27[a]	3+	176.8 (C+), 169.4, 150.8, 149.6, 148.2, 141.2, 140.3, 139.4, 137.2, 135.6	176.0, 138.7, 145.8, 141.9, 178.2
NH+, NH+, NH+, CH	36	4+		150.2, 149.0, 146.0, 148.9, 201.2
NH+, NH+, NH+, NH+	37	5+		125.8, 165.0, 143.9, 155.7, 231.0

[a] (a) Spectrum taken at −60 °C. (b) Spectrum taken at 0 °C.

occurs by nucleophilic attack at the 1-position of the naphthyl group. This implies a greater contribution from resonance structure **35b**, instead of structure **35c** (the structure with greater charge separation).
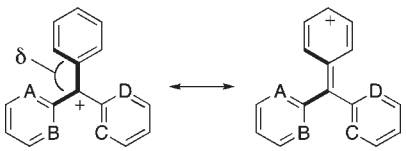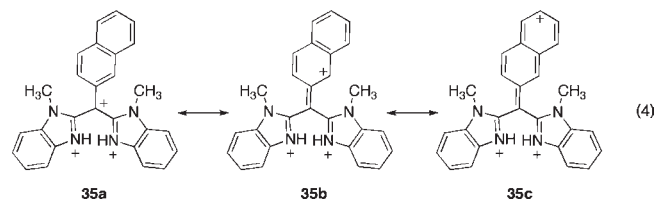

To gain further insight into these reactions, low temperature ^{13}C NMR experiments were done. Compound **4** was ionized in FSO₃H−SbF₅−SO₂ClF at −60 °C, and the observed spectrum is consistent with the formation of the tricationic species **27** (Table 2). For comparison, the DFT calculated spectrum of trication **27** is in reasonably good agreement with the results from solution (for complete assignments of ^{13}C signals, see the

Supporting Information). It is notable that the para and ortho carbons are significantly deshielded. This is consistent with the charge delocalization driven by charge−charge repulsive effects. The dicationic ion **26** and the trityl cation (**25**)[24] were also studied in solution by low temperature ^{13}C NMR, with comparison to calculated spectra. Interestingly, the chemical shift at the methine carbon moves progressively downfield from the monocationic trityl cation (**25**), to the dication (**26**), and to the trication (**27**). This is an indication that charge delocalization becomes enhanced with increasing charge. The tetra- and pentacationic structures (**36**, **37**) were also calculated, and the results show further deshielding of the para-position and shielding of the methine carbon. While the trityl cation has a calculated chemical shift of δ 144 at the para position of the phenyl ring, the pentacation **37** has a calculated chemical shift of δ 231 at the para position of the phenyl ring.

As a measure of charge delocalization in these systems, natural bond order (NBO) charges, bond lengths, and dihedral angles were analyzed from the calculated structures. In a series of related

Table 3. Calculated Properties of Isoelectric Ions 25−27 and 36,37

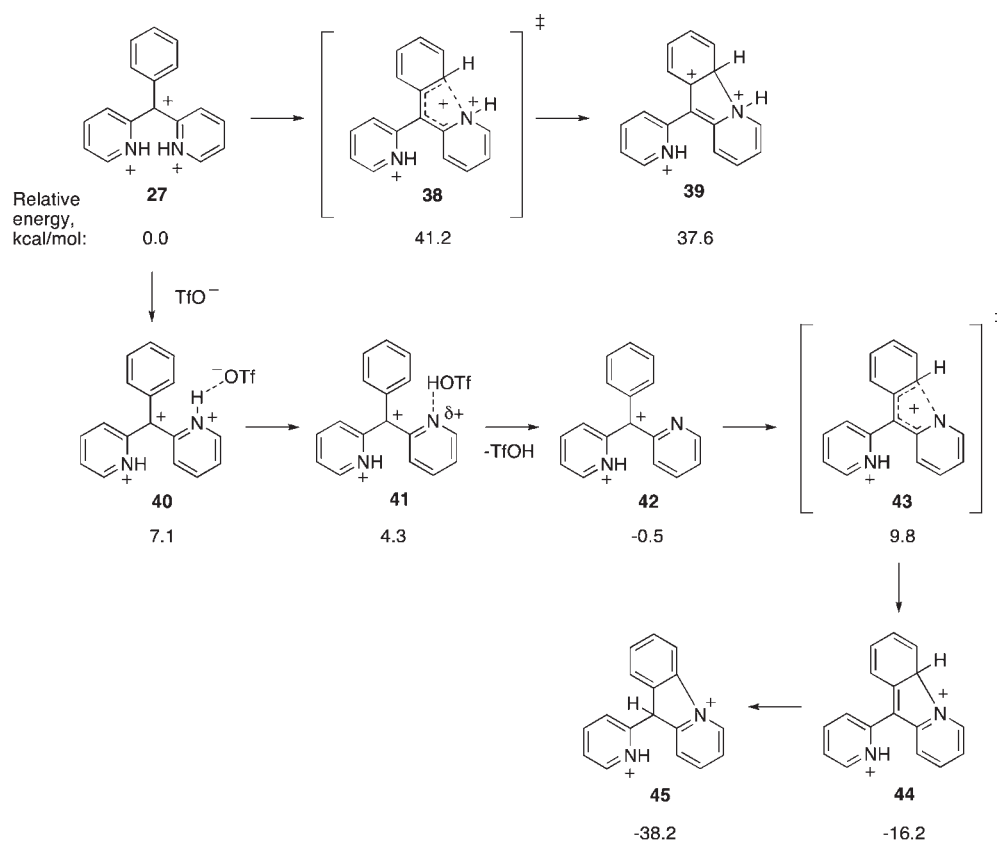| structure | charge | NBO charge | | dihedral angle, δ | C−C bond length (methine-ipso), Å |
		C-methine	C-para		
25	1+	+0.24	−0.15	33.2°	1.441
26	2+	+0.15	−0.10	31.1°	1.429
27	3+	+0.12	0.00	24.0°	1.402
36	4+	−0.01	+0.10	19.5°	1.394
37	5+	−0.14	+0.20	11.2°	1.391

Figure 4. Calculated structures related to the cyclization of trication 27.

structures, ^{13}C NMR chemical shifts may be roughly correlated to charge densities.[25] Down field chemical shifts (or deshielding) often correspond to electron-deficient carbon atoms.[25] Within the isoelectronic series from the trityl cation (**25**) to the pentacation (**37**), experimental and calculated NMR spectral data suggest that the carbocationic center moves progressively from the methine carbon to the para position of the phenyl ring. The calculated NBO charges also show this trend (Table 3). Remarkably, there is almost a complete transfer of positive charge from the methine carbon to the *para*-carbon. The methine carbon

carries a +0.24 NBO charge in the trityl cation (**25**) and a −0.14 NBO charge in the pentacation (**37**), while the *para*-carbon carries a −0.15 NBO charge in **25** and a +0.20 NBO charge in **37**. As the positive charge is moved to the para position, there is also increasing double bond character between the methine carbon and the phenyl ring. This is apparent from the decreasing bond dihedral angle (δ) and C−C bond length as charge is added to the system. Thus, the trityl cation **25** has a dihedral angle of 33.2° and C−C bond length of 1.441 Å, while the pentacation **37** has a dihedral bond angle of 11.2° and C−C bond length of 1.391 Å.

The dihedral angle and NBO charge are strongly correlated to the overall charge on the cationic structure. Increasing charge leads to progressively greater positive charge at the *para*-carbon, while simultaneously increasing electron density at the methine carbon (evident from the negative NBO charges). Although it might be expected that a carbocationic center would exhibit increasing positive charge as neighboring groups become more electron deficient, the opposite occurs in this case. The increasing charge of the *N*-heterocycles leads to charge migration across the phenyl ring to the remote para position (maximizing the charge—charge separation).

As described in Table 1, compound **4** reacts in CF$_3$SO$_3$H to give the pyrido[1,2-*a*]indole derivative (**16**) in the absence of an arene nucleophile. Because ionization of **4** should provide trication **27**, theoretical calculations were also done to study the cyclization of the tricationic species **27** (Figure 4). Calculations suggest that direct cyclization of the trication **27** is unlikely, as the transition state **38** leading to **39** is estimated to be 41 kcal/mol above **27**. The cyclized trication **39** itself is 38 kcal/mol higher in energy. A lower energy pathway was found involving initial deprotonation at the pyridinium ring, proceeding through two minima (**40** and **41**) and giving dication **42** in a slightly exothermic step. Cyclization then occurs with a barrier of 9.8 kcal/mol (**43**), and it gives stabilized species **44** and **45**. Upon basic workup, cation **45** provides the observed product **16**. Although triflate normally would not be expected to deprotonate a pyridinium ring, the high charge density of the trication **27** must lead to enhanced acidity of the pyridinium hydrogen. Previous studies have shown superelectrophiles to possess highly acidic protons.[26] With trication **27**, the carbocationic site cannot readily lead to a deprotonation equilibrium, so instead the pyridinium ring undergoes deprotonation.

Ionization of compound **4** in FSO$_3$H—SbF$_5$—SO$_2$ClF gives NMR spectral data that differs somewhat from the calculated spectrum for trication **27**. While experimental NMR spectra often differ slightly from the calculated spectra, the present case may be the result of an equilibrium between trication **27** and the dication **42**. Rapid proton transfer should average the spectral data from **27** and **42**, and this would account for the differences between the calculated and experimental spectra for trication **27**. As shown in Table 2, the experimental data for the compound **4** ionization product, presumably trication **27**, showed a methine resonance at δ 176.8 and *para*-carbon at δ 169.4. The calculated spectrum for **27** has a methine resonance at δ 176.0 and *para*-carbon at δ 178.2. When dication **42** was studied computationally, the calculated spectrum has a methine resonance at δ 179.1 and *para*-carbon at δ 161.6 (for a full list of peaks, see the Supporting Information). If a numerical average is made from the calculated chemical shift values of trication **27** and dication **42**, then an averaged spectrum should have methine resonance at δ 177.6 and *para*-carbon at δ 169.9. These averaged values are very close to the experimentally determined values from ionization of **4** in magic acid. Moreover, the calculated energies of **27** and **42** are within 0.5 kcal/mol, suggesting a significant concentration of these two species from the low temperature ionization.

This raises an obvious question: could all of the chemistry simply involve equilibria between dications? This question was examined computationally by considering the step in which the alcohol ionizes to the carbocation. Assuming the alcohol group must be protonated for ionization, this means the dicationic intermediate **46** would of necessity be involved in the chemistry. However, calculations indicate that **46** is about 35 kcal/mol less
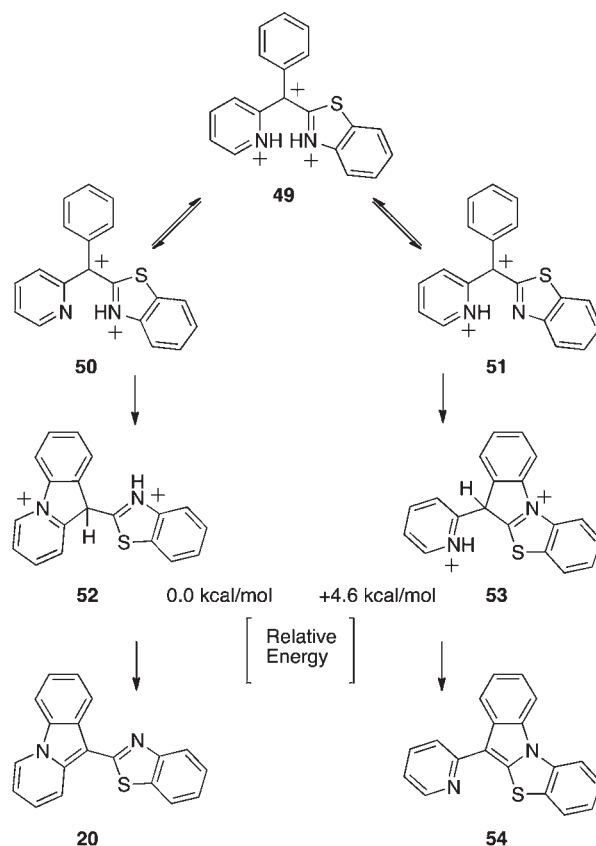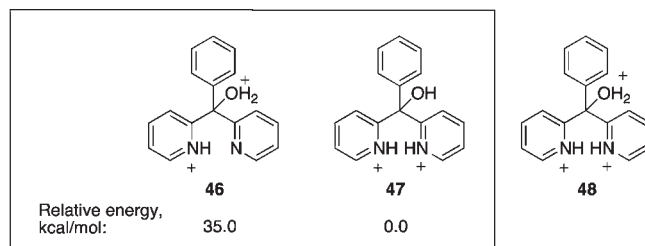

Figure 5. Cyclization of trication **46** to compounds **20** and **51**.

stable than the dication in which both pyridyl rings are protonated (**47**). This strongly suggests the formation of the tricationic oxonium ion **48**, leading to the proposed tricationic superelectrophile **27**.

As described in Table 1, compound **15** reacts in superacid to give the pyrido[1,2-*a*]indole **20**. This product is somewhat surprising, as a dicationic cyclization might be expected to cyclize into the benzothiazole ring. Assuming ionization of **15** leads to the trication **49**, deprotonation could lead to either **50** or **51**, but only dication **50** should lead to product **20** (Figure 5). However, the pK_a data for the parent heterocycles suggest that the benzothiazole ring should be more acidic (pK_a for pyridine 5.2; pK_a for benzothiazole 1.2).[27] This apparent inconsistency may be explained by considering the stabilities of the intermediates **52** and **53**. DFT calculations have shown that cyclization through the pyridine ring leads to an intermediate (**52**) that is 4.6 kcal/mol more stable than a similar intermediate with benzothiazole cyclization (**53**). Likewise, product **20** is almost 4 kcal/mol more stable than its isomer **54**.

■ CONCLUSIONS

We have studied the superacid-promoted reactions of a series of triarylmethanols, which generate tricationic intermediates. As compared to analogous mono- and dicationic species, the tricationic intermediates exhibit new reactions resulting from the effects of the closely oriented positive charges. These effects include the tendency for cationic charge to "migrate" across a phenyl ring and the tendency for neighboring protons to exhibit very high acidities. The migration of charge across organic structures is important in material science applications and in the design of organic-based electronics. Our results show that densely charged structures may have high charge mobilities. As a consequence, these tricationic superelectrophiles react with arene nucleophiles at a remote site. Without a nucleophilic reactant, cyclizations occur to provide novel N-heterocyclic products. The functionalized heterocycles are produced in good to excellent yields. Computational studies indicate that this chemistry arises from the deprotonation of an unusually acidic pyridinium ring.

■ ASSOCIATED CONTENT

Ⓢ Supporting Information. Detailed experimental procedures, characterization data, ^1H and ^{13}C NMR spectra for new compounds, ^{13}C NMR spectra for ions **26** and **27**, computational methods and results, and crystallographic data for compounds **11** and **18**. This material is available free of charge via the Internet at http://pubs.acs.org.

■ AUTHOR INFORMATION

Corresponding Author
dklumpp@niu.edu

■ ACKNOWLEDGMENT

■ REFERENCES

(1) Olah, G. A.; Germain, A.; Lin, H. C.; Forsyth, D. *J. Am. Chem. Soc.* **1975**, *97*, 2928–2929.

(2) Olah, G. A.; Klumpp, D. A. *Superelectrophiles and Their Chemistry*; Wiley: New York, 2008.

(3) (a) Prakash, G. K. S.; Rawdah, T. N.; Olah, G. A. *Angew. Chem., Int. Ed. Engl.* **1983**, *22*, 390–401. (b) Ito, S.; Morita, N.; Asao, T. *Bull. Chem. Soc. Jpn.* **2000**, *73*, 1865–1874. (c) Head, N. J.; Prakash, G. K. S.; Bashir-Hashemi, A.; Olah, G. A. *J. Am. Chem. Soc.* **1995**, *117*, 12005–12006. (d) Rathore, R.; Burns, C. L.; Green, I. A. *J. Org. Chem.* **2004**, *69*, 1524–1530. (e) Reddy, V. P.; Rasul, G.; Prakash, G. K. S.; Olah, G. A. *J. Org. Chem.* **2003**, *68*, 3507–3510. (f) See also: Pagni, R. M. *Tetrahedron* **1984**, *49*, 4161–4215.

(4) For recent examples of reactive tricationic species, see: (a) Ohwada, T.; Yamagata, N.; Shudo, K. *J. Am. Chem. Soc.* **1991**, *113*, 1364–1373. (b) Kurouchi, H.; Sugimoto, H.; Otani, Y.; Ohwada, T. *J. Am. Chem. Soc.* **2010**, *132*, 807–815. (c) Zhang, Y.; Sheets, M. R.; Raja, E. K.; Boblak, K. J.; Klumpp, D. A. *J. Am. Chem. Soc.* **2011**, *133*, 8467–8469.

(5) Crystallographic data are found in the Supporting Information.

(6) (a) Posselt, K. *Arzneim. Forsch.* **1978**, *28*, 1056–1065. (b) See also: Alarcon, H. A. R.; Soldatenkov, A. T.; Soldatova, S. A.; Samalyoa, A. I.; Obando, H. U.; Prostakov, N. S. *Khim. Geterotsikl. Soedin.* **1993**, 1233–1238.

(7) Decomposition products are obtained.

(8) Sommer, J.; Bukala, J. *Acc. Chem. Res.* **1993**, *26*, 370–376.

(9) Zhao, Y.; Truhlar, D. *Theor. Chem. Acc.* **2008**, *120*, 215–241.

(10) *Jaguar*, version 7.7; Schrodinger, LLC: New York, 2010.

(11) Dunning, T. H. *J. Chem. Phys.* **1989**, *90*, 1007–1023.

(12) Woon, D. E.; Dunning, T. H. *J. Chem. Phys.* **1993**, *98*, 1358–1371.

(13) Marten, B.; Kim, K.; Cortis, C.; Friesner, R. A.; Murphy, R. B.; Ringnalda, M. N.; Sitkoff, D.; Honig, B. *J. Phys. Chem.* **1996**, *100*, 11775–11788.

(14) Lira, A. L.; Zolotukhin, M.; Fomina, L.; Fomine, S. *J. Phys. Chem. A* **2007**, *111*, 13606–13610.

(15) Frisch, M. J. T.; et al. *Gaussian 03*, revision D.02; Gaussian, Inc.: Wallingford, CT, 2004.

(16) Stephens, P. J.; Devlin, F. J.; Chabalowski, C. F.; Frisch, M. J. *J. Phys. Chem.* **1994**, *98*, 11623–11627.

(17) Kutzelnigg, W.; Fleischer, U.; Schindler, M. In *NMR, Basic Principles and Progress*; Diehl, P., Fluck, E., Günther, H., Kosfield, R., Seelig, J., Eds.; Springer-Verlag: Berlin, 1990; Vol. 23, pp 165−262.

(18) Glendening, E. D.; Badenhoop, J. K.; Reed, A. E.; Carpenter, J. E.; Bohmann, J. A.; Morales, C. M.; Weinhold, F. *NBO 5.0*; Theoretical Chemistry Institute, University of Wisconsin, Madison, WI, 2001; http://www.chem.wisc.edu/∼nbo5.

(19) Mackie, I. D.; DiLabio, G. A. *J. Phys. Chem. A* **2008**, *112*, 10968–10976.

(20) Nilsson Lill, S. O. *J. Mol. Graphics Modell.* **2010**, *29*, 178–187.

(21) (a) Ohwada, T.; Okabe, K.; Ohta, T.; Shudo, K. *Tetrahedron* **1990**, *46*, 7539–7555. (b) Shudo, K.; Ohta, T.; Okamoto, T. *J. Am. Chem. Soc.* **1981**, *103*, 645–653. (c) Nakamura, S.; Sugimoto, H.; Ohwada, T. *J. Am. Chem. Soc.* **2007**, *129*, 1724–1732. (d) O'Connor, M. J.; Boblak, K. N.; Topinka, M. J.; Kindelin, P. J.; Briski, J. M.; Zheng, C.; Klumpp, D. A. *J. Am. Chem. Soc.* **2010**, *132*, 3266–3267.

(22) Nelson, K. L.; Brown, H. C. *J. Am. Chem. Soc.* **1951**, *73*, 5605–5607.

(23) Olah, G. A. *Acc. Chem. Res.* **1971**, *4*, 240–248.

(24) Abarca, B.; Asensios, G.; Ballesteros, R.; Luna, C. *Tetrahedron Lett.* **1986**, *27*, 5657–5660.

(25) (a) Forsyth, D. A.; Sandel, B. B. *J. Org. Chem.* **1980**, *45*, 2391–2394. (b) Forsyth, D. A.; Spear, R. J.; Olah, G. A. *J. Am. Chem. Soc.* **1976**, *98*, 2512–2518.

(26) (a) Nenajdenko, V. G.; Shevchenko, N. E.; Balenkova, E. S. *Chem. Rev.* **2003**, *103*, 229–282. (b) Olah, G. A.; Grant, J. L.; Spear, R. J.; Bollinger, J. M.; Serianz, A.; Sipos, G. *J. Am. Chem. Soc.* **1976**, *98*, 2501. (c) Larsen, J. W.; Bouis, P. A. *J. Am. Chem. Soc.* **1975**, *97*, 6094–6102. (d) Olah, G. A.; Calin, M. *J. Am. Chem. Soc.* **1968**, *90*, 4672–4675. (e) Olah, G. A.; Reddy, V. P.; Rasul, G.; Prakash, G. K. S. *J. Am. Chem. Soc.* **1999**, *121*, 9994–9998.

(27) (a) Perrin, D. D. *Dissociation Constants of Organic Bases in Aqueous Solution*; Butterworths: London; 1965. (b) Eicher, T.; Hauptmann, S. *The Chemistry of Heterocycles*; Wiley-VHC: Weinheim, 2003.